Erratum: Equation of state and correlation functions of hypernuclear matter within the lowest order constrained variational method [Phys. Rev. C 100, 044314 (2019)]

M. Shahrbaf, H. R. Moshfegh, and M. Modarres

(Received 30 July 2026; published 16 September 2026)

DOI: 10.1103/ngfy-7khm

During a recent review and extension of our lowest-order constrained variational (LOCV) numerical implementation, we identified an error in the channel-selection procedure used in the original article. The Pauli-exclusion restrictions appropriate to identical nucleon pairs were inadvertently also imposed on the ΛN channels. Since a Λ hyperon and a nucleon are distinguishable particles, these restrictions should not be applied to the ΛN pair. Consequently, several physically allowed ΛN partial-wave channels, including the ${}^1S_0$, ${}^3P_0$, ${}^3P_1$, ${}^1D_2$, and ${}^3P_2$-${}^3F_2$ channels, were omitted from the numerical calculation.

Because the LOCV correlation functions are determined self-consistently through a common normalization constraint, this channel-selection error affected the channel decomposition of the two-body interaction energy, the correlation functions, and other derived numerical results. The analytical LOCV formalism presented in the original article remains unchanged.

All references cited in the main text, figures, and tables remain valid and unchanged. Figure 1 and Tables I–III of the original article are unaffected. However, because the channel-selection error modified the self-consistent determination of the correlation functions and the energy per particle, Figs. 2–12 and Tables IV and V are affected.

In some cases, the resulting numerical changes are very small. Nevertheless, to ensure the accuracy and completeness of the published results, we have recalculated and reproduced all figures and tables that depend on the LOCV numerical calculation. The corrected figures and tables, together with the corresponding corrections to the main text where required, are presented below.

Although the qualitative conclusions of the original article remain largely unchanged, the corrected results exhibit a common quantitative trend: the effects associated with the inclusion of Λ hyperons are generally reduced, both in the energy per baryon and in most of the correlation functions. A notable channel-dependent exception is the $N\Lambda\,{}^1P_1$ correlation function, which remains suppressed over a wider radial interval and therefore exhibits a longer healing distance in the corrected calculation. One of the most significant corrections is presented in Table IV, in which all physically allowed partial-wave channels are now included for the $p\Lambda$ and $n\Lambda$ interactions. The corresponding channel contributions and the total two-body interaction energy have therefore changed.

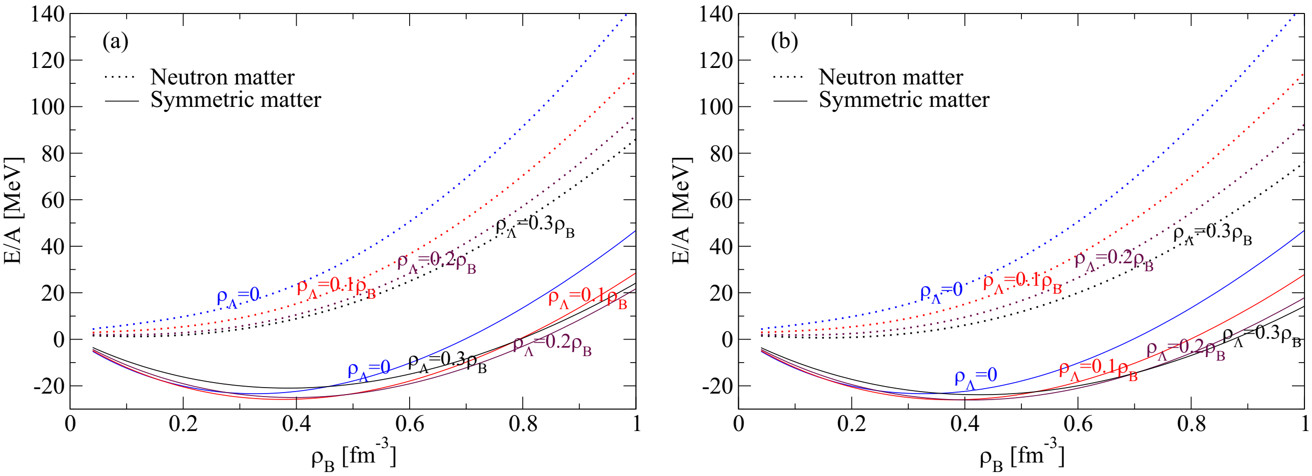

FIG. 2. Corrected version of Fig. 2 of the original article. The equation of state of hypernuclear matter as a function of baryon density for different x_Λ. The solid lines show the case of symmetric nuclear matter which includes Λ, while the dotted lines correspond to the case of $x_p = 0$, by using (a) the repulsive odd-state part of the $\Lambda\Lambda$ interaction and (b) the attractive odd-state part of the $\Lambda\Lambda$ interaction.

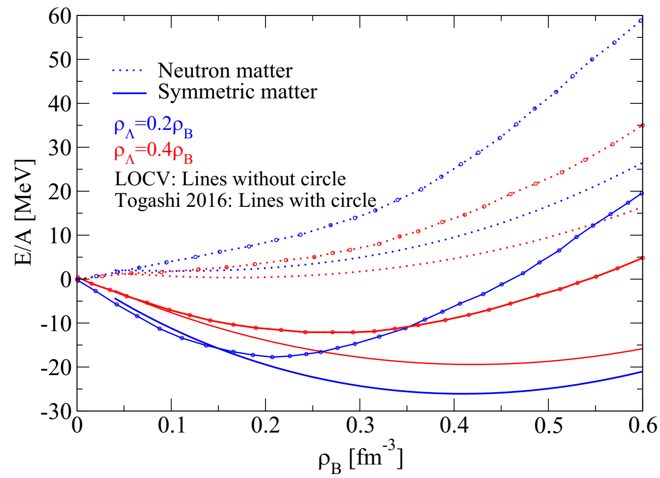

FIG. 3. Corrected version of Fig. 3 of the original article. The comparison of the EoS for hypernuclear matter calculated within the LOCV method and the variational method used in the work of Togashi *et al*. [53]. In both methods, the same interactions for NY and YY have been used.

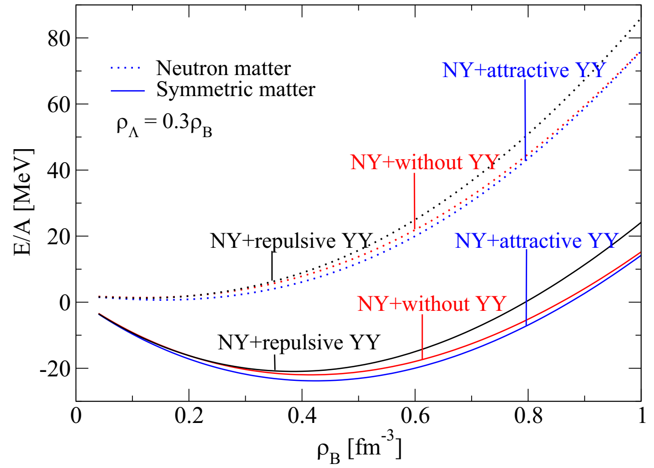

FIG. 4. Corrected version of Fig. 4 of the original article. The equation of state of hypernuclear matter as a function of baryon density. The cases which include an attractive $\Lambda\Lambda$ interaction and a repulsive one as well as the case in which we removed the $\Lambda\Lambda$ interaction are compared. The solid lines show the case of symmetric nuclear matter which includes Λ, while the dotted lines correspond to the case of $x_p = 0$.

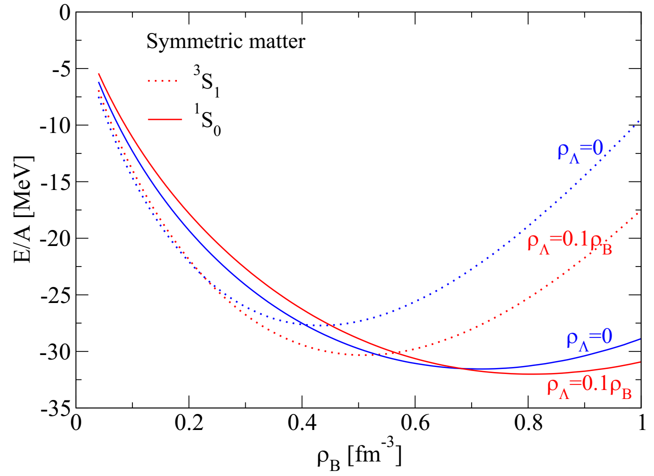

FIG. 5. Corrected version of Fig. 5 of the original article. The comparison of ${}^1S_0$ and ${}^3S_1$ channel contributions to the binding energy for nuclear matter and hypernuclear matter.

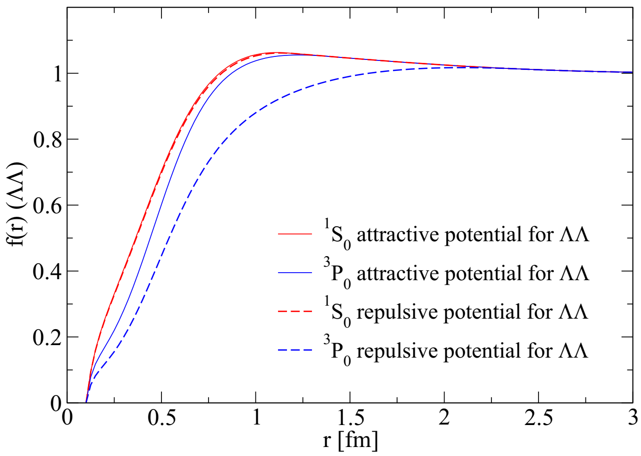

FIG. 6. Corrected version of Fig. 6 of the original article. The correlation functions for both attractive and repulsive potentials in the $^1S_0$ and $^3P_0$ channels at $\rho_B = 0.17$ fm^{-3} and $\rho_\Lambda = 0.3\rho_B$. All the curves are plotted for the symmetric nuclear matter, i.e., $x_p = x_n$.

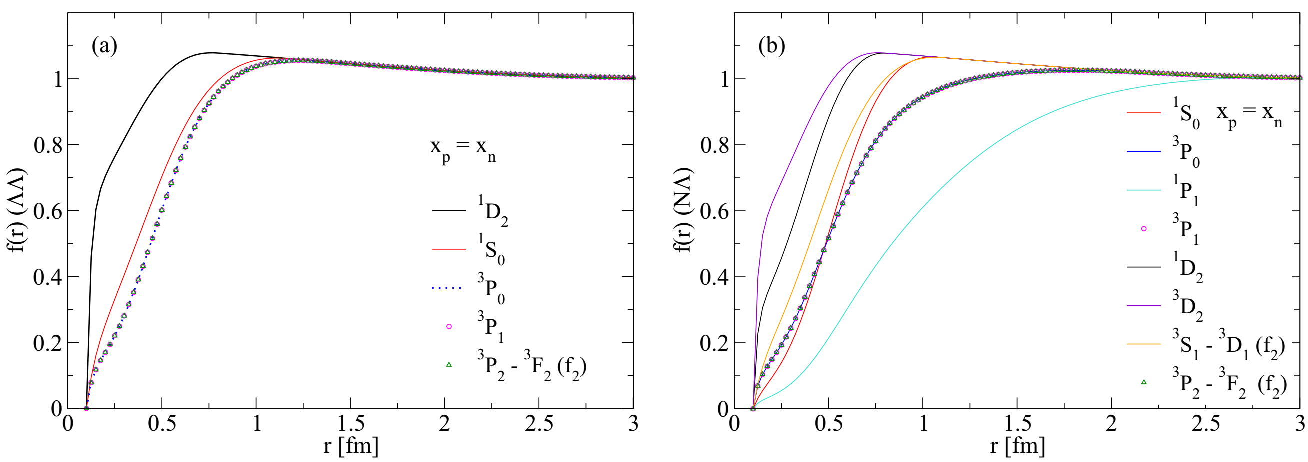

FIG. 7. Corrected version of Fig. 7 of the original article. The correlation functions using the attractive potential for the odd part in all interacting channels for $J \leqslant 2$ at $\rho_B = 0.17$ fm^{-3} and $\rho_\Lambda = 0.3\rho_B$, for (a) $\Lambda\Lambda$ interaction and (b) $N\Lambda$ interaction.

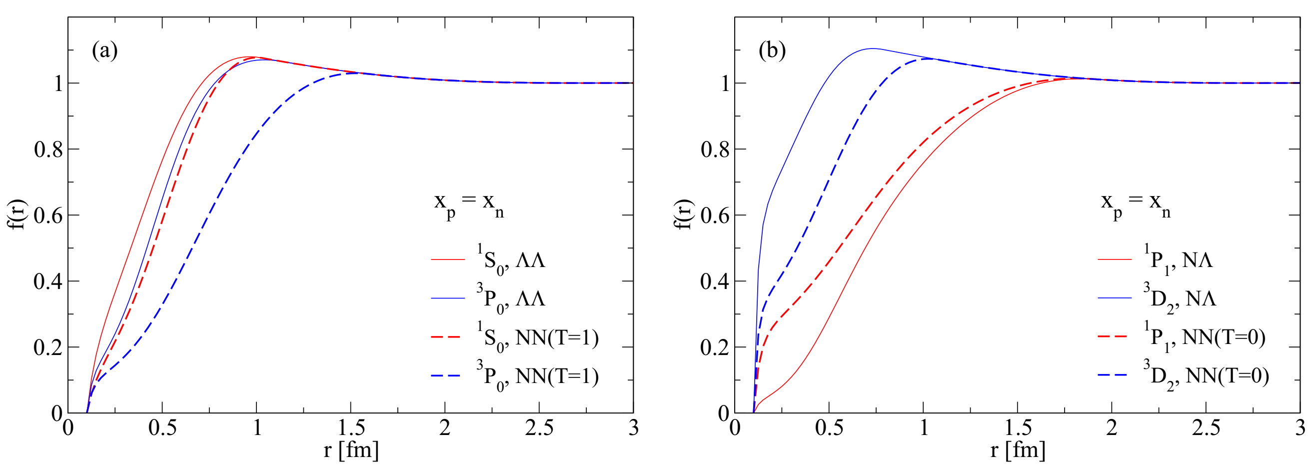

FIG. 8. Corrected version of Fig. 8 of the original article. The two-body correlation function at $\rho_B = 0.30$ fm^{-3}, $\rho_\Lambda = 0.005\rho_B$, and $x_p = x_n$. (a) The correlation function of the $\Lambda\Lambda$ interaction using the attractive potential for the odd part compared with those of the NN interaction with $T = 1$. (b) The correlation function of the $N\Lambda$ interaction using the attractive potential for the odd part compared with those of the NN interaction with $T = 0$.

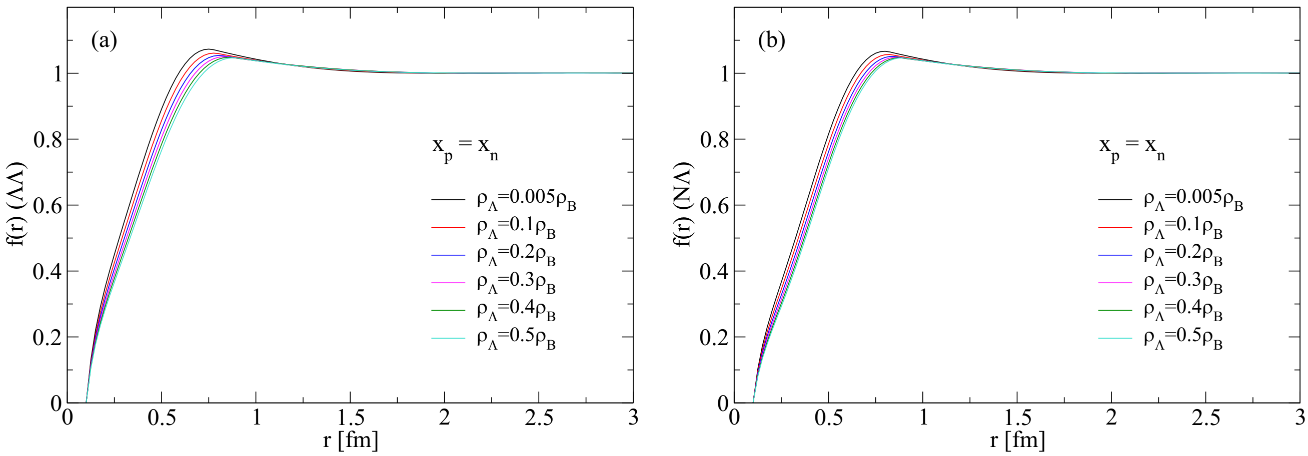

FIG. 9. Corrected version of Fig. 9 of the original article. The comparison of correlation functions at $\rho_B = 0.80$ fm^{-3} and $x_p = x_n$ for different Λ fractions: (a) $\Lambda\Lambda$ interaction for the $^1S_0$ channel and (b) $N\Lambda$ interaction for the $^3S_1$ channel.

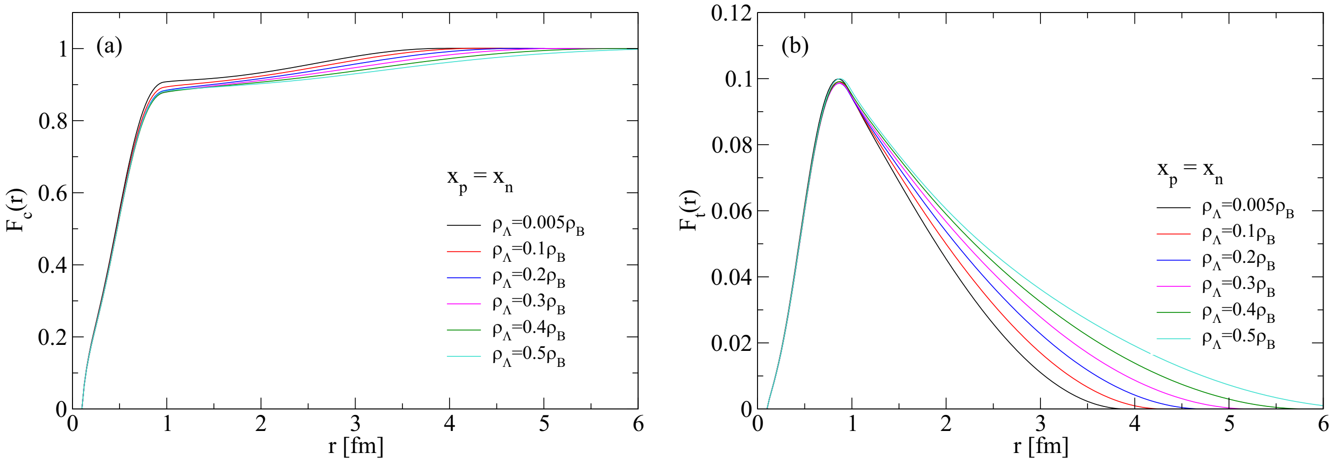

FIG. 10. Corrected version of Fig. 10 of the original article. The comparison of $^3S_1 - {}^3D_1$ correlation functions at $\rho_B = 0.17$ fm^{-3} and $x_p = x_n$ for different Λ fractions: (a) central and (b) tensor correlation function.

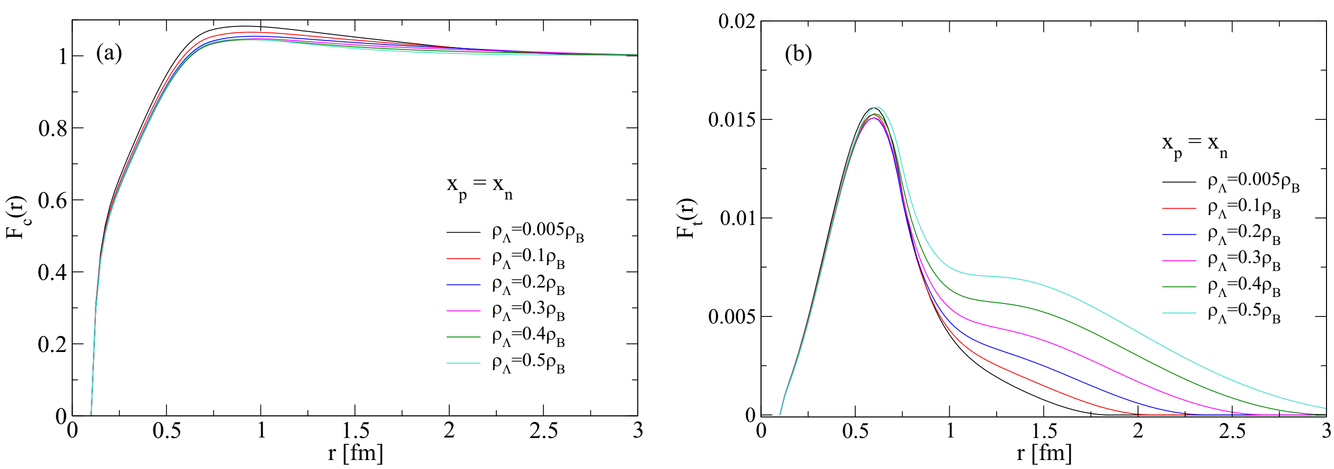

FIG. 11. Corrected version of Fig. 11 of the original article. The comparison of $^3P_2 - {}^3F_2$ correlation functions at $\rho_B = 0.17$ fm^{-3} and $x_p = x_n$ for different Λ fractions: (a) central and (b) tensor correlation function.

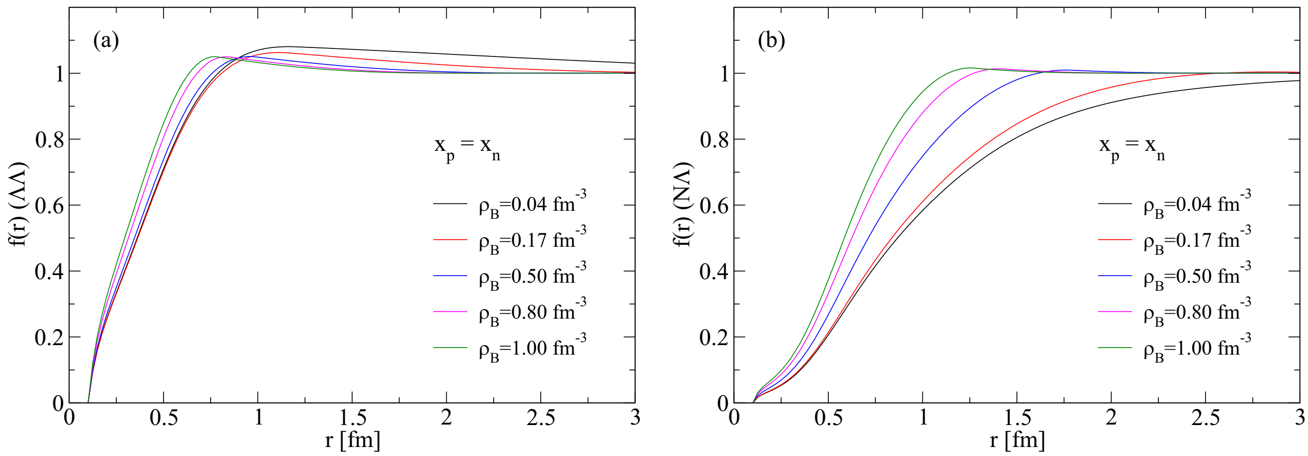

FIG. 12. Corrected version of Fig. 12 of the original article. The comparison of hyperonic correlation functions at $\rho_\Lambda = 0.3\rho_B$ and $x_p = x_n$ for different ρ_B: (a) $\Lambda\Lambda$ interaction for the $^1S_0$ channel and (b) $N\Lambda$ interaction for the $^1P_1$ channel.

TABLE IV. Corrected version of Table IV of the original article. Comparison of channel breakdown of energy (MeV) for hypernuclear matter and nuclear matter up to $J = 2$ at $\rho_B = 0.3$ fm^{-3} and $\rho_\Lambda = 0.3\rho_B$ when $x_p = x_n$.

Channel	pp	nn	$\Lambda\Lambda$	$np1$	$np0$	$p\Lambda$	$n\Lambda$	$\sum M_T$	No Λ
$^1S_0$	−4.453	−4.489	−0.680	−4.597		−2.460	−2.461	−19.14	−24.126
$^3P_0$	−0.994	−0.995	−0.087	−0.915		0.033	0.033	−2.925	−5.291
$^1P_1$					3.298	1.216	1.216	5.73	7.246
$^3P_1$	2.835	2.832	−0.261	2.719		0.099	0.099	8.323	19.075
$^3S_1$					−15.511	−4.746	−4.748	−25.005	−26.061
$^3D_1$					1.023	−0.118	−0.118	0.787	2.555
$^1D_2$	−0.864	−0.865	−0.086	−0.828		−0.239	−0.239	−3.121	−6.064
$^3D_2$					−3.601	−0.199	−0.199	−3.999	−8.193
$^3P_2$	−2.147	−2.161	−0.435	−2.114		0.165	0.164	−6.528	−14.759
$^3F_2$	−0.175	−0.175	−0.007	−0.153		−0.009	−0.009	−0.528	−1.225
Total	−5.798	−5.853	−1.556	−5.888	−14.791	−6.258	−6.262	−46.406	−56.843

TABLE V. Corrected version of Table V of the original article. Comparison of the reproduced energies calculated within the LOCV method with those of hypernuclei determined experimentally [67] or calculated so as to reproduce reasonably the existing data for the Λ-binding energy [51].

x_Λ	x_p/x_n	E_{LOCV} (MeV)	Hypernucleus	$E_{\mathrm{hypernuclei}}$ (MeV)
$\frac{1}{6}$	$\frac{2}{3}$	−5.9250	$^{6}_{\Lambda}$He	−3.29 [51]
$\frac{2}{6}$	1	−4.6614	$^{6}_{\Lambda\Lambda}$He	−7.25 [51]
$\frac{2}{7}$	$\frac{2}{3}$	−5.2187	$^{7}_{\Lambda\Lambda}$He	−8.47 [51]
$\frac{1}{8}$	$\frac{3}{4}$	−6.9222	$^{8}_{\Lambda}$Li	−9.30 [51]
$\frac{2}{8}$	1	−6.1006	$^{8}_{\Lambda\Lambda}$Li	−12.10 [51]
$\frac{1}{9}$	1	−7.4475	$^{9}_{\Lambda}$Be	−6.64 [51]
$\frac{2}{10}$	1	−7.0511	$^{10}_{\Lambda\Lambda}$Be	−15.05 [51]
$\frac{1}{89}$	$\frac{39}{49}$	−12.9697	$^{89}_{\Lambda}$Y	$\simeq -23$ [67]
$\frac{1}{139}$	$\frac{57}{81}$	−13.4482	$^{139}_{\Lambda}$La	$\simeq -24$ [67]
$\frac{1}{208}$	$\frac{82}{125}$	−13.8244	$^{208}_{\Lambda}$Pb	$\simeq -26$ [67]

Accordingly, the sentence beginning with “which results in a total energy of” in the fourth paragraph of the right column on p. 6 of the original article must be corrected. The value −19.99 MeV should be replaced by −21.82 MeV as a consequence of the corrected two-body interaction energy.

In the paragraph discussing Fig. 6 at the end of p. 7 and beginning of p. 8 of the original article, the sentence beginning with “This is a good test” should be replaced by: “This is a good test for the results of our method, because as the figure shows and we expected, the CFs in the $^1S_0$ channel are almost unchanged because the same even-state $\Lambda\Lambda$ interaction is used in both calculations. However, in the $^3P_0$ channel, the CF clearly has a shorter range for the attractive potential.”

In the paragraph following Fig. 8 on p. 8 of the original article, the final two sentences should be replaced by the following: “As can be seen in Fig. 8(a), and in the $^3D_2$ channel of Fig. 8(b), the hyperonic CFs have a shorter range than the corresponding nucleonic CFs. However, in the $^1P_1$ channel of Fig. 8(b), the $N\Lambda$ CF has a longer range than the NN CF with $T = 0$. Therefore, the relative ranges of the hyperonic and nucleonic CFs are channel dependent and cannot be attributed to the larger hyperon mass alone.”

Although the $N\Lambda$ $^1P_1$ channel was already present in the original calculation, its correlation function is coupled to all other channels through the common LOCV normalization constraint and its associated Lagrange multiplier. Restoring the previously omitted $N\Lambda$ channels therefore readjusts its variational solution. Because this channel probes the strongly repulsive singlet-odd component of the adopted $N\Lambda$ interaction, it is particularly sensitive to this readjustment. Compared with the original result, the corrected correlation is lower over a wider range and heals at a larger distance, indicating stronger pair suppression. Consistent with this behavior, at the state point considered in Table IV, the combined $p\Lambda + n\Lambda$ contribution increases from approximately 0.19 to 2.432 MeV, while the total $^1P_1$ contribution increases from 3.43 to 5.73 MeV.

In the last paragraph of the Conclusion section on p. 10 of the original article, the sentence “The results show that hyperonic correlation functions have a shorter range in comparison with the nucleonic one.” should be replaced by: “The results show that the relative ranges of the hyperonic and nucleonic correlation functions are channel dependent. In most of the channels considered, the hyperonic correlation functions have a shorter range than the corresponding nucleonic ones; however, the $N\Lambda$ correlation function in the $^1P_1$ channel has a longer range than the corresponding NN correlation function with $T = 0$.”

We are deeply grateful to Makoto Oka for bringing the missing ΛN channels to our attention and for his careful and insightful discussions, which were essential for identifying and correcting the numerical error reported in this Erratum. M.S. also sincerely thanks Emiko Hiyama for the invitation to visit the RIKEN Nishina Center as a visiting researcher and gratefully acknowledges the warm hospitality of the Few-body Systems in Physics Laboratory, RIKEN Nishina Center, during her stay. M.S. has been supported by the National Science Centre, Poland (NCN), under SONATINA 7 Grant No. 2023/48/C/ST2/00297.

[51] E. Hiyama, M. Kamimura, T. Motoba, T. Yamada, and Y. Yamamoto, Four-body cluster structure of $A = 7 - 10$ double-Λ hypernuclei, Phys. Rev. C **66**, 024007 (2002).

[53] H. Togashi, E. Hiyama, Y. Yamamoto, and M. Takano, Equation of state for neutron stars with hyperons using a variational method, Phys. Rev. C **93**, 035808 (2016).

[67] O. Hashimoto and H. Tamura, Spectroscopy of Λ hypernuclei, Prog. Part. Nucl. Phys. **57**, 564 (2006).